# ENTANGLEMENT OF TRAPPED IONS

C. BECHER [1] *†, J. BENHELM [1], D. CHEK-AL-KAR [1], M. CHWALLA [1], H. HÄFFNER [1,2], W. HÄNSEL [1], T. KÖRBER [1], A. KREUTER [1], G.P.T. LANCASTER [1], T. MONZ [1], E.S. PHILLIPS [1], U.D. RAPOL [1], M. RIEBE [1], C.F. ROOS [1,2], C. RUSSO [1], F. SCHMIDT-KALER [1] ‡, AND R. BLATT [1,2]

[1] *Institut für Experimentalphysik, Universität Innsbruck, Technikerstraße 25, A-6020 Innsbruck, Austria*

[2] *Institut für Quantenoptik und Quanteninformation, Österreichische Akademie der Wissenschaften, Otto-Hittmair-Platz 1, A-6020 Innsbruck, Austria*

Entanglement, its generation, manipulation, measurement and fundamental understanding is at the very heart of quantum mechanics. We here report on the creation and characterization of entangled states of up to 8 trapped ions, the investigation of long-lived two-ion Bell-states and on experiments towards entangling ions and photons.

## 1. Introduction

In 1935 Erwin Schrödinger wrote in a seminal paper introducing the phrase *entanglement*: "I would call entanglement not one but rather the characteristic trait of quantum mechanics, the one that enforces its entire departure from classical lines of thought."[1]. Entangled particles are described by a *common* wavefunction where individual particles are not independent of each other but where their quantum properties are inextricably interwoven. Since the pioneering work of Freedman and Clauser[2] and Aspect[3] there has been a huge progress in generating and characterizing entangled states (see e.g. the review by Weinfurter[4]). Here we describe the creation and mea-

*E-mail: christoph.becher@uibk.ac.at

†Present address: Fachrichtung Technische Physik, Universität des Saarlandes, Postfach 151150, D-66041 Saarbrücken, Germany

‡Present address: Abteilung Quanten-Informationsverarbeitung, Universität Ulm, Albert-Einstein-Allee 11, D-89069 Ulm, Germany

surement of entangled states of trapped ions. In particular, we investigate three different aspects: 1. The robustness of entangled states by observing the lifetime of two-ion Bell-states, 2. Creation and measurement of many-particle entangled states, and 3. Proposed experiments on entanglement of a single ion with photons.

Regarding the robustness of entanglement, it is common belief among physicists that entangled states of quantum systems loose their coherence rather quickly, as stated e.g. by Yu and Eberly: "Our intuition strongly suggests that a specified entanglement, as a nonlocal property of a composed quantum system, should be very fragile under the influence of the environment"[5]. The reason for the fragility of entangled states is that any interaction with the environment which distinguishes between the entangled sub-systems collapses the quantum state[6]. We here investigate entangled states of two trapped $Ca^+$ ions and observe robust entanglement lasting for more than 20 seconds[7]. This observation is not only of importance for fundamental science but also for the emerging field of quantum information since entanglement is believed to be the ingredient making a quantum computer[8] much more powerful than any classical machine. Because of the fragility of entanglement physicists widely assume that it is very hard -if not impossible- to construct such a quantum computer[9]. Furthermore, the decoherence properties of entangled states play a central role in understanding the emergence of our classical world from quantum mechanics, as stated by Raimond et al. "Entanglement is also essential to understand decoherence, the process accounting for the classical appearance of the macroscopic world."[10]. Consequently, there is a strong interest and need in generating entangled states and investigating their coherence properties in well controlled physical systems.

As of today, entanglement properties of two and three particles have been studied extensively and are very well understood. Entanglement of four ions[11] and five photons[12] was demonstrated experimentally. However, both creation and characterization of entanglement become exceedingly difficult for multi–particle systems. Thus the availability of such multi–particle entangled states together with the full information on these states in form of their density matrices creates a test-bed for theoretical studies of multi-particle entanglement, in particular for the development of entanglement measures. Here, we use as a convenient tool for classification of genuine multipartite entanglement the instrument of entanglement witnesses[13,14,15]. Among the various kinds of entangled states, the W–state[16,17,18] plays an important role since its entanglement is maximally

persistent and robust even under particle losses. Such states are central as a resource to the new fields of quantum information processing[19] and multi-party quantum communication[20,21]. Here we report the deterministic generation of W–type entangled states with four to eight trapped ions[22]. We obtain the maximum possible information on these states by performing full characterization via state tomography[23]. Moreover, we prove in a detailed analysis that they carry genuine four-, five-, six-, seven- and eight–particle entanglement, respectively.

Finally, scaling-up of quantum processors might require the possibility to transfer quantum information stored in internal atomic states to a light field by coupling to a cavity mode[24], thereby entangling atomic and photonic states. The interconnection of multiple atom-cavity systems via photonic channels then allows for transport of quantum information within distributed quantum networks[25]. Realization of a quantum network requires an interface between atoms as static quantum bits and photons as moving quantum bits. Such an interface could be based on the deterministic coupling of a single atom or ion to a high finesse optical cavity[26,27]. Trapped and laser-cooled ions are ideally suited systems for the realization of such atom-photon interfaces[28]. Recently, probabilistic entanglement between a trapped ion's hyperfine states and the polarization state of a spontaneously emitted photon has been demonstrated[29]. Here, we propose to deterministically entangle an ion and a photon by driving adiabatic Raman passages[28] and convert the resulting photon state from a Fock basis to a time-bin-entangled basis[30].

## 2. Experimental Setup

All experiments are performed with an ion–trap quantum processor[31]. We trap strings of up to eight $^{40}Ca^{+}$ ions in a linear Paul trap. Superpositions of the $S_{1/2}$ ground state and the metastable $D_{5/2}$ state of the $Ca^{+}$ ions (lifetime of the $|D\rangle$–level: $\tau \approx 1.16$ s) represent the qubits. Each ion–qubit in the linear string is individually addressed by a series of tightly focused laser pulses on the $|S\rangle \equiv S_{1/2}(m_j = -1/2) \longleftrightarrow |D\rangle \equiv D_{5/2}(m_j = -1/2)$ quadrupole transition employing narrowband laser radiation near 729 nm. Doppler cooling and subsequent sideband cooling prepare the ion string in the ground state of the center–of–mass vibrational mode. Optical pumping initializes the ions' electronic qubit states in the $|S\rangle$ state. After preparing a desired state with a series of laser pulses, the quantum state is read out with a CCD camera.

## 3. Lifetime of entangled states

A sequence of three laser pulses addressing the ions individually creates the entangled Bell state $|\Psi\rangle = (|SD\rangle + |DS\rangle)/\sqrt{2}$.[23]. Via state tomography[23] we find an overlap of the experimentally generated state with the ideal one (the fidelity) of up to 96%. For this Bell state we obtain coherence times of more than 1 s, consistent with the fundamental limit set by the spontaneous decay from the $D_{5/2}$-level[23]. This observation is due to the fact that the constituents of the superposition have the same energy and are thus insensitive to fluctuations common to both ions (e.g. laser frequency and magnetic field fluctuations). Similar results have been obtained with Bell states encoded in hyperfine levels of Beryllium ions[32,33].

In a further experiment, we extend the lifetime of the entangled state by more than one order of magnitude by encoding the Bell state in Zeeman sublevels of the ground state. In particular, we coherently transfer - just after the entangling operation - the population of the $|D_{5/2}, m_J = -1/2\rangle$ state to the $|S_{1/2}, m_J = +1/2\rangle \equiv |0\rangle$ state, while leaving the $|S_{1/2}, m_J = -1/2\rangle \equiv |1\rangle$ population untouched. The fidelity of the resulting Bell state $|\Psi'\rangle = (|01\rangle + |10\rangle)/\sqrt{2}$ is 89 % where the loss of 7 % is due to imperfect transfer pulses. For investigating decoherence, we insert a variable delay time before analyzing the state $|\Psi'\rangle$. After a delay of 1 s, full state tomography reveals that the fidelity of the entangled state is still 86 %. Since the tomographic reconstruction of the full density matrix requires many experimental cycles ($\approx 1000$), it is of advantage to employ a fidelity measure that is based on a single density matrix element and thus is easier to access. Indeed, to determine a lower bound of the fidelity $F_{\min}$, it is sufficient[7,11] to measure the density matrix element $\langle 01|\rho|10\rangle = 1/2F_{\min}$.We plot the experimentally determined values for $F_{\min}$ in Fig. 1 and find that the fidelity is larger than 0.5 for up to 20 s; thus at least up to this time the ions were still entangled[11].

We considered the following reasons for the observed decay of entanglement: slow fluctuations of the magnetic field gradient which affect the ions differently, heating of the ion crystal, residual light scattering, and collisions. The latter three were excluded experimentally.[7]A magnetic field gradient across the ion trap lifts the energy degeneracy of the two parts of the superposition by $\Delta E = h \times 30$ Hz such that the relative phase $\phi$ of the superposition evolves as $\phi(t) = \Delta E t/\hbar$ . Thus relative fluctuations of the gradient by $10^{-3}$ within the measurement time of up to 90 minutes per data point could explain the observed decay rate of $|\langle 01|\rho|10\rangle|$. Generally,

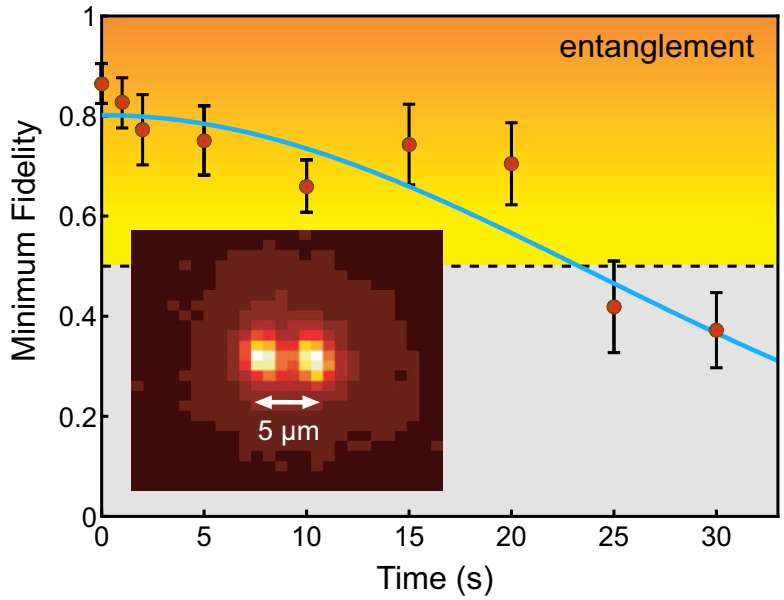


Figure 1. Minimum fidelity of the Bell state as a function of the delay time as inferred from the density matrix element $\langle 01|\rho|10\rangle$. A fidelity of more than 0.5 indicates the presence of entanglement. The inset shows the fluorescence image of two $Ca^+$ ions which were entangled in this measurement.

a slow dephasing mechanism such as fluctuations of the magnetic field gradient leads to a Gaussian decay of the coherence. A Gaussian fit to the data in Fig. 1 yields a time constant of 34(3) s for the loss of coherence of the entangled state.

Previous experiments with single trapped $Be^+$-ions have demonstrated that single particle coherence can be kept for more than 10 minutes[34]. Here we show that also entangled states can be preserved for many seconds: the two-ion Bell states in our investigations outlive the single particle coherence time of about 1 ms in our system[35] by more than 4 orders of magnitude. Even in the presence of an environment hostile for a single atom quantum memory, the coherence is preserved in a decoherence free subspace[32].

## 4. Multi-particle entanglement

An $N$–particle W–state

$$|W_N\rangle = \left(|D\cdots DDS\rangle + |D\cdots DSD\rangle + |D\cdots DSDD\rangle + \cdots + |SD\cdots D\rangle\right)/\sqrt{N}$$

consists of a superposition of $N$ states where exactly one particle is in the $|S\rangle$–state while all other particles are in $|D\rangle$[16,17]. W–states are genuine $N$–particle entangled states of special interest: their entanglement is not only maximally persistent and robust under particle losses[36], but also immune against global dephasing, and rather robust against bit flip noise. In addition, for larger numbers of particles, W–states may lead to stronger non–classicality[37] than GHZ–states[38] and may be used for quantum communication[20,21].

The W–states are efficiently generated by sharing one motional quantum between the ions with partial swap–operations[18]. With the procedure outlined in Tab. 1 we create $|W_N\rangle$–states ($N \leq 8$) in about $500 - 1000$ $\mu$s.

Full information on the $N$–ion entangled state is obtained via quantum state reconstruction by expanding the density matrix in a basis of observables[23] and measuring the corresponding expectation values. We use $3^N$ different bases and repeat the experiment 100 times for each basis. For $N = 8$, this amounts to 656 100 experiments and a total measurement time of 10 hours. To obtain a positive semi–definite density matrix $\rho$, we follow the iterative procedure outlined by Hradil *et al.*[39] for performing a maximum–likelihood estimation of $\rho$.

The reconstructed density matrix for $N = 6$ is displayed in Fig. 2. To retrieve the fidelity $F = \langle W_N|\rho|W_N\rangle$, we adjust the local phases such that $F$ is maximized. The local character of those transformations implies that the amount of the entanglement present in the system is not changed. We obtain fidelities $F_4 = 0.85, F_5 = 0.76$, $F_6 = 0.79$, $F_7 = 0.76$ and $F_8 = 0.72$ for the 4,5,6,7 and 8–ion W–states, respectively.

We investigate the influence of quantum projection noise on the reconstructed density matrix and quantities derived from it by means of a Monte Carlo simulation. Starting from the reconstructed density matrix, we simulate up to 100 test data sets taking into account the major experimental uncertainty, i.e. quantum projection noise. Then the test sets are analyzed and we can extract probability distributions for all observables from the resulting density matrices.

We analyze the entangled states by investigating (i) the presence of genuine multipartite entanglement, (ii) the distillability of multipartite entanglement and (iii) entanglement in reduced states of two qubits. For this, we associate each particle $k$ of a state $\rho$ with a (possibly spatially separated) party $A_k$. We shall be interested in different aspects of entanglement between parties $A_k$, i.e. the non–locality of the state $\rho$.

In order to show the presence of multipartite entanglement, we use

Table 1. Creation of a $|W_N\rangle$–state ($N = \{6, 7, 8\}$). First we initialize the ions via sideband cooling and optical pumping in the $|0, SS\cdots S\rangle$–state where we use the notation $|n, x_N x_{N-1}\cdots x_1\rangle$. $n$ describes the vibrational quantum number of the ion motion and $x_i$ their electronic state. We then prepare the $|0, DDD\cdots D\rangle$–state with $N$ $\pi$–pulses on the carrier transition applied to ions #1 to #$N$, denoted by $R_n^C(\theta = \pi)$. Then this state is checked for vanishing fluorescence with a photomultiplier tube. The same is done after trying to drive a $\pi$–pulse on the blue sideband on ion #1 to ensure that the ion crystal is in the motional ground state. After this initialisation, we transform the state to $|0, SDD\cdots D\rangle$ with a carrier pulse and start the entanglement procedure in step (1). This is carried out by moving most of the population to the $|1, DDD\cdots D\rangle$ with a blue sideband pulse of length $\theta_n = \arccos(1/\sqrt{n})$ leaving the desired part back in $|0, SDD\cdots D\rangle$. Finally, we use $N-1$ blue sideband pulses ($R_n^+(\theta_n)$) of pulse length $\theta_n = \arcsin(1/\sqrt{n})$ such that at each step we split off a certain fraction of the wave packet. Note that for an ion string in the ground state, blue–sideband pulses acting on an ion in the D–state have no effect. For $N = \{4, 5\}$ we do not check the fluorescence, combine steps $i1$ and $i3$ and omit step $i2$.

| | |
|---|---|
| | $\|0, SSS\cdots S\rangle$ |
| (i1) | $\xrightarrow{R_N^C(\pi)R_{N-1}^C(\pi)\cdots R_1^C(\pi)}$ |
| | $\|0, DDD\cdots D\rangle$ |
| | Check state via fluorescence |
| (i2) | $\xrightarrow{R_1^+(\pi)}$ |
| | $\|0, DDD\cdots D\rangle$ |
| | Check state via fluorescence |
| (i3) | $\xrightarrow{R_N^C(\pi)}$ |
| | $\frac{1}{\sqrt{N}}\|0, SDD\cdots D\rangle$ |
| (1) | $\xrightarrow{R_N^+(2\arccos(1/\sqrt{N}))}$ |
| | $\frac{1}{\sqrt{N}}\|0, SDD\cdots D\rangle + \frac{\sqrt{N-1}}{\sqrt{N}}\|1, DDD\cdots D\rangle$ |
| (2) | $\xrightarrow{R_{N-1}^+(2\arcsin(1/\sqrt{N-1}))}$ |
| | $\frac{1}{\sqrt{N}}\|0, SDD\cdots D\rangle + \frac{1}{\sqrt{N}}\|0, DSD\cdots D\rangle + \frac{\sqrt{N-2}}{\sqrt{N}}\|1, DDD\cdots D\rangle$ |
| ⋮ | ⋮ |
| | $\frac{1}{\sqrt{N}}\|0, SDD\cdots D\rangle + \frac{1}{\sqrt{N}}\|0, DSD\cdots D\rangle + \cdots + \frac{1}{\sqrt{N}}\|1, DDD\cdots D\rangle$ |
| (N) | $\xrightarrow{R_1^+(2\arcsin(1/\sqrt{1}))}$ |
| | $\frac{1}{\sqrt{N}}\|0, SDD\cdots D\rangle + \frac{1}{\sqrt{N}}\|0, DSD\cdots D\rangle + \cdots + \frac{1}{\sqrt{N}}\|0, DDD\cdots S\rangle$ |

the method of entanglement witnesses[13,14,15]. An entanglement witness for multipartite entanglement is an observable with a positive expectation value on all biseparable states. Thus a negative expectation value proves the presence of genuine multipartite entanglement. A typical witness for

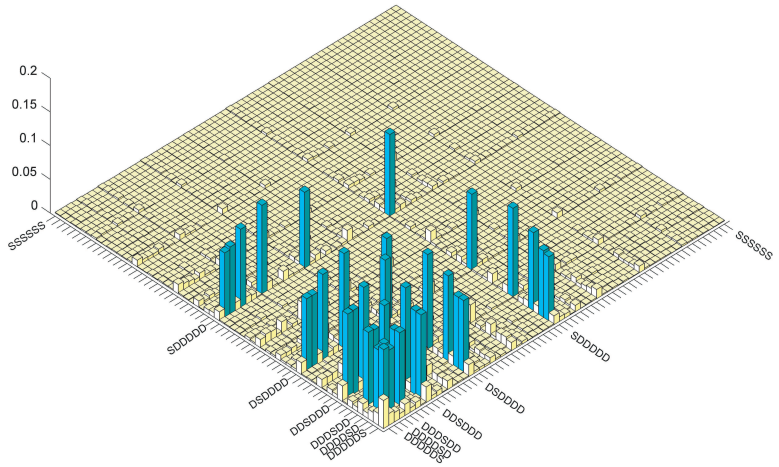


Figure 2. Absolute values of the reconstructed density matrix of a $|W_6\rangle$–state as obtained from quantum state tomography.

the states $|W_N\rangle$ would be[15]

$$\mathcal{W}_N = \frac{N-1}{N} - |W_N\rangle\langle W_N|. \tag{1}$$

This witness detects a state as entangled if the fidelity of the W–state exceeds $(N-1)/N$. However, more sophisticated witnesses can be constructed, if there is more information available on the state under investigation than only the fidelity. To do so, we add other operators to the witness in Eq. 1[22] which take into account that certain biseparable states can be excluded on grounds of the measured density matrix. Table 2 lists the expectation values for these advanced witnesses. The negative expectation values prove that in our experiment genuine four, five, six, seven and eight qubit entanglement has been produced.

Secondly, we consider the question whether one can use many copies of the state $\rho$ to distill one pure multipartite entangled state $|\psi\rangle$ by local means, i.e. whether entanglement contained in $\rho$ is qualitatively equivalent to multiparty pure state entanglement. Technically, multipartite distillability follows from the possibility to generate maximally entangled singlet states $|\psi^-\rangle = (|DS\rangle - |SD\rangle)/\sqrt{2}$ between any pair of parties $A_k, A_l$ by local means[40]. The latter can be readily shown for all reconstructed density matrices. Performing measurements of $\sigma_z$ on all particles except $k, l$ and

restricting to outcomes $P_0 = |D\rangle\langle D|$ in all cases results in the creation of a two–qubit state $\rho_{kl}$. The density operator $\rho_{kl}$ is distillable entangled if the concurrence $C$, a measure for two–qubit entanglement[41], is non–zero. This is the case for all $k, l$ (see Tab. 2), which implies that $\rho_N$ is multiparty distillable entangled.

Thirdly, we investigate bipartite aspects of multiparticle entanglement[42], in particular the entanglement in the reduced states of two qubits. For W–states this is of special interest, since for these states all reduced density operators of two particles are entangled, and the entanglement is in fact maximal[22]. We investigate the bipartite entanglement by tracing out all but particles $k, l$ and obtain the reduced density operators $\rho'_{kl}$. From these density matrices we can now calculate the concurrence $C'_{kl} = C(\rho'_{kl})$ as a measure for the entanglement. For all $N$, we find that all reduced density operators are entangled (see Tab. 2). Note that the previous results (presence of multipartite entanglement and distillability) also imply that $\rho$ is inseparable and in fact distillable with respect to any bipartition for all $N$.

Table 2. Entanglement properties of $\rho_N$. First row: Fidelity after properly adjusting local phases. Second row: Expectation value of the witnesses $\tilde{\mathcal{W}}_N$ (for $N = 8$ we used additionally local filters). Third and fourth row: minimal and average concurrence between two qubits after $\sigma_z$–measurement on the remaining $(N-2)$ qubits. Fifth and sixth row: minimal and average concurrence between two qubits after discarding the remaining $(N-2)$ qubits. For completeness we also analyzed the data published previously for $N = 3$.

| | $N=3$ | $N=4$ | $N=5$ | $N=6$ | $N=7$ | $N=8$ |
|---|---|---|---|---|---|---|
| $F$ | 0.824 | 0.846 (11) | 0.759 (7) | 0.788(5) | 0.763 (3) | 0.722 (1) |
| $\mathrm{tr}(\tilde{\mathcal{W}}_N\rho_N)$ | −0.532 | −0.460 (31) | −0.202 (27) | −0.271 (31) | −0.071 (32) | −0.029 (8) |
| $\min(C_{kl})$ | 0.724 | 0.760 (34) | 0.605 (23) | 0.567 (16) | 0.589 (9) | 0.536 (8) |
| $\bar{C}$ | 0.776 | 0.794 (23) | 0.683 (15) | 0.677 (11) | 0.668 (5) | 0.633 (3) |
| $\min(C'_{kl})$ | 0.294 | 0.229 (21) | 0.067 (12) | 0.049 (4) | 0.035 (4) | 0.022 (3) |
| $\bar{C}'$ | 0.366 | 0.267 (12) | 0.162 (6) | 0.124(3) | 0.091 (2) | 0.073 (1) |

Finally, we address the scalability of our approach. Four major sources for deviations from the ideal W–states are found: addressing errors, imperfect optical pumping, non–resonant excitations and frequency stability of the qubit–manipulation–laser[22]. All of them are purely technical and thus represent no fundamental obstacle for increasing the number of particles. Also the required blue sideband pulse area for a $|W\rangle$–state scales only with $\log N$ (see Tab. 1) while the time for a pulse with given area is proportional to the square root of the ion crystal's mass. Thus the overall favorable scaling behaviour of $\sqrt{N}\log N$ opens a way to study large scale entanglement

experimentally.

## 5. Towards ion-photon entanglement

In order to realize a deterministic ion-photon coupling we have constructed a setup featuring a linear ion trap inside a high-finesse optical cavity. The cavity has been realized as near-concentric cavity (19.92 mm mirror spacing, 10 mm radius of curvature high quality mirrors) with a mode waist of 13.1 $\mu$m and a finesse of 80.000 at 854 nm, yielding the coupling parameters $(g, \kappa, \gamma) = 2\pi(1.28, 0.047, 23)$ MHz and a cooperativity of $C = 1.5$. Emission of a single photon into the cavity mode will be achieved by adiabatic Raman passage involving an excitation pulse on the $Ca^+$ $S_{1/2}$ - $P_{3/2}$ transition (393 nm) and cavity tuning to the $P_{3/2}$ - $D_{5/2}$ transition (854 nm)[28]. Numerical simulations of the photon emission process yield a probability for emitting a single photon per pump pulse of about 90% with repetition rates of 20 kHz (pulse width 50 $\mu$s) and vanishing two-photon probability $g^2(0) < 10^{-4}$. The transmission of the generated photons out of the cavity output coupler is expected to be $> 50\%$.

For investigations on entangling the internal electronic state of the ion and the cavity mode we can use the single photon emission scheme[28]. The static qubit can be encoded in superpositions of either $S_{1/2}$ and $D_{5/2}$ states or of the Zeeman sublevels of the $S_{1/2}$ ground state. Driving a Raman passage transfers part of such a superposition to an excitation of the cavity mode, i.e. a transfer from a basis $\{|S\rangle, |D\rangle\}$ or $\{|S\rangle, |S'\rangle\}$ to the photon Fock basis $\{|0\rangle, |1\rangle\}$. For our parameters, the Raman process works coherently with a 70% probability, i.e. in 7 out of 10 cases there is no spontaneous emission during the Raman passage which could destroy the coherence of the process. We therefore anticipate that the planned experiments should yield almost deterministic entanglement between atomic and photonic states.

The experimental scheme starts with a preparation of a certain superposition state of the ion. After emission of a photon, entanglement between the internal electronic states and the photon state has to be verified. We propose to convert the $\{|0\rangle, |1\rangle\}$ photon basis into a time-bin basis $\{t_1, t_2\}$ where the photon state is encoded in two well defined time intervals[30]. In this scheme, one has to drive two Raman passages starting from the two electronic levels in which the superposition state is encoded. The cavity output is coupled into an optical fiber interferometer where a fiber switch directs the first pulse into a long fiber arm and the second pulse into a short

fiber arm, with a length difference equal to the pulse separation. Both fiber arms are then recombined in a beamsplitter. If one fiber arm contains a phase shifter one can observe interference effects. Entanglement between atomic states and photonic states can now be verified by preparation of superpositions of atomic states with different phases, transfer and observation of interference fringes depending on the phase shift in one interferometer arm. The long duration of the photon wavepackets here requires a fiber length of more than 10 km, certainly a challenging task. However, if the cavity coupling can be increased by new techniques (e.g. by the combination of miniaturized ion traps and fiber cavities) the requirements for the experiment are easier to fulfill: both the repetition rate of emission increases and the required fiber length decreases such that the signal to noise ratio for correlation counts increases.

## Acknowledgments

We gratefully acknowledge support by the European Commission (CONQUEST (MRTN-CT-2003-505089) and QGATES (IST-2001-38875) networks), by the ARO (No. DAAD19-03-1-0176), by the Austrian Fonds zur Förderung der wissenschaftlichen Forschung (FWF, SFB15), and by the Institut für Quanteninformation GmbH. H.H. acknowledges funding by the Marie-Curie-program of the European Union. T.K. acknowledges funding by the Lise-Meitner program of the FWF. C. Russo acknowledges support by Fundação para a Ciência e a Tecnologia (Portugal) under the grant SFRH/BD/6208/2001.

## References

1. E. Schrödinger, *Proceedings of the Cambridge Philosophical Society* **31**, 555 (1935).
2. S.J. Freedman and J.F. Clauser, *Phys. Rev. Lett.* **28**, 938 (1972).
3. A. Aspect, P. Grangier, and G. Roger, *Phys. Rev. Lett.* **47**, 460 (1981).
4. H. Weinfurter, *J. Phys. B: At. Mol. Opt. Phys.*, **38**, S579 (2005).
5. T. Yu and J.H. Eberly, *Phys. Rev. B* **66**, 193306 (2002).
6. W.H. Zurek, *Physics Today* **44**, 36 (1991).
7. H. Häffner *et al*,*Appl. Phys. B* **81**, 151(2005).
8. M.A. Nielsen and I.L. Chuang, *Quantum Computation and Quantum Information*, (Cambridge University Press, Cambridge, 2000).
9. S. Haroche and J.M. Raimond, *Physics Today* **49**, 51 (1996).
10. J.M. Raimond, M. Brune, and S. Haroche, *Rev. Mod. Phys.* **73**, 565 (2001).
11. C.A. Sackett *et al.*, *Nature* **404**, 256(2000).
12. Z. Zhao *et al.*, *Nature* **430**, 54(2004).

13. M. Horodecki, P. Horodecki, and R. Horodecki, *Phys. Lett. A* **223**, 1(1996).
14. B.M. Terhal, *Phys. Lett. A* **271**, 319(2000).
15. M. Bourennane *et al.*, *Phys. Rev. Lett.* **92**, 087902 (2004).
16. W. Dür, G. Vidal, and J.I. Cirac, *Phys. Rev. A* **62**, 062314 (2000).
17. A. Zeilinger, M.A. Horne, and D.M. Greenberger, *NASA Conf. Publ.* **3135**, pp 73–81 (1992).
18. C.F. Roos *et al.*, *Science* **304**, 1478(2004).
19. C.H. Bennett and D.P. DiVincenzo, *Nature* **404**, 247(2000).
20. H. Buhrman, W. van Dam, P. Høyer, and A. Tapp, *Phys. Rev. A* **60**, 2737(1999).
21. J. Joo, J. Lee, J. Jang, and Y.-J. Park, *arXiv:quant-ph/*0204003; J. Joo, Y.-J. Park, J. Lee, J. Jang, and I. Kim, *J. Korean Phys. Soc.* **46**, 763(2005).
22. H. Häffner *et al.*, *submitted to Nature*, (2005).
23. C.F. Roos *et al.*, *Phys. Rev. Lett.* **92**, 220402 (2004).
24. A.S. Parkins, P. Marte, P. Zoller, O. Carnal, and H.J. Kimble *Phys. Rev. A* **51**, 1578 (1995).
25. J.I. Cirac, P. Zoller, H.J. Kimble, and H. Mabuchi *Phys. Rev. Lett* **78**, 3221 (1997).
26. G.R. Guthöhrlein, M. Keller, K. Hayasaka, W. Lange, and H. Walther, *Nature* **414**, 49 (2001).
27. A.B. Mundt *et al.*,*Phys. Rev. Lett* **89**, 103001 (2002).
28. C. Maurer, C. Becher, C. Russo, J. Eschner, and R. Blatt, *New J. Phys.* **6**, 94 (2004).
29. B.B. Blinov, D.L. Moehring, L.-M. Duan, and C. Monroe, *Nature* **428**, 153 (2004).
30. J. Brendel, N. Gisin, W. Tittel, and H. Zbinden, *Phys. Rev. Lett* **82**, 2594 (1999).
31. F. Schmidt-Kaler *et al.*, *Appl. Phys. B* **77**, 789 (2003).
32. D. Kielpinski *et al.*, *Science* **291**, 1013 (2001).
33. R. Ozeri *et al.*, *Phys. Rev. Lett.* **95**, 030403 (2005).
34. J.J. Bollinger, D.J. Heinzen, W.M. Itano, S.L. Gilbert, and D.J. Wineland, *IEEE Trans. Instrum. Meas.* **40**, 126 (1991).
35. F. Schmidt-Kaler *et al.*, *J. Phys. B: At. Mol. Opt. Phys.* **36**, 623 (2003).
36. H.J. Briegel, and R. Raussendorf, *Phys. Rev. Lett.* **86**, 000910 (2001).
37. A. Sen(De), U. Sen, M. Wiesniak, D. Kaszlikowski, and M. Zukowski, *Phys. Rev. A* **68**, 062306 (2003).
38. D.M. Greenberger, M. Horne, and A. Zeilinger, in *Bell's Theorem, Quantum theory, and conceptions of the universe*, edited by M. Kafatos (Kluwer Academic, Dordrecht, 1989).
39. Z. Hradil, J. Reháček, J. Fiurášek, and M. Ježek, *Lect. Notes Phys.* **649**, 59(2004).
40. W. Dür and J.I. Cirac, *Phys. Rev. A* **61**, 042314 (2000).
41. W.K. Wootters, *Phys. Rev. Lett.* **80**, 2245(1998).
42. W. Dür and J.I. Cirac, *Journal of Physics A: Mathematical and General* **34**, 6837(2001).